HHS Public Access

Author manuscript

Environ Microbiol. Author manuscript; available in PMC 2019 April 01.

Published in final edited form as:

Environ Microbiol. 2018 April ; 20(4): 1419–1435. doi:10.1111/1462-2920.14048.

Ethanolamine is a Valuable Nutrient Source that Impacts *Clostridium difficile* Pathogenesis

Kathryn L. Nawrocki[1], **Daniela Wetzel**[1], **Joshua B. Jones**[1], **Emily C. Woods**[1], and **Shonna M. McBride**[1,#]

[1]Department of Microbiology and Immunology, and Emory Antibiotic Resistance Center, Emory University School of Medicine, Atlanta, GA, USA

SUMMARY

Clostridium (Clostridioides) difficile is a gastrointestinal pathogen that colonizes the intestinal tract of mammals and can cause severe diarrheal disease. Although *C. difficile* growth is confined to the intestinal tract, our understanding of the specific metabolites and host factors that are important for the growth of the bacterium is limited. In other enteric pathogens, the membrane-derived metabolite, ethanolamine (EA), is utilized as a nutrient source and can function as a signal to initiate the production of virulence factors. In this study, we investigated the effects of ethanolamine and the role of the predicted ethanolamine gene cluster (*CD1907–CD1925*) on *C. difficile* growth. Using targeted mutagenesis, we disrupted genes within the *eut* cluster and assessed their roles in ethanolamine utilization, and the impact of *eut* disruption on the outcome of infection in a hamster model of disease. Our results indicate that the *eut* gene cluster is required for the growth of *C. difficile* on ethanolamine as a primary nutrient source. Further, the inability to utilize ethanolamine resulted in greater virulence and a shorter time to morbidity in the animal model. Overall, these data suggest that ethanolamine is an important nutrient source within the host and that, in contrast to other intestinal pathogens, the metabolism of ethanolamine by *C. difficile* can delay the onset of disease.

Keywords

Clostridium difficile; *Clostridioides*; *difficile*; ethanolamine; metabolism; ethanolamine metabolism; ethanolamine utilization; *eut*; *tcdA*; *tcdB*; virulence; pathogenesis; branched-chain amino acids (BCAA)

INTRODUCTION

Clostridium (Clostridioides) difficile is a common nosocomial pathogen that can cause severe intestinal infections. *C. difficile* pathogenesis results primarily from the actions of two large exotoxins, TcdA and TcdB, that destroy host intestinal tissues (Lyerly et al., 1985; Lyras et al., 2009; Kuehne et al., 2010). This host cell destruction is thought to liberate cell

[#]Corresponding author. Mailing address: Department of Microbiology and Immunology, Emory University School of Medicine, 1510 Clifton Rd, Atlanta, GA 30322. Phone: (404) 727-6192. Fax: (404) 727-8250. shonna.mcbride@emory.edu.

The authors have no conflicts of interest to declare.

contents that provide additional nutrients to support bacterial growth. However, little is known about how cell contents and other metabolites available in the intestine impact growth, or how the diverse metabolic pathways of *C. difficile* contribute to colonization and virulence.

A number of overlapping regulatory factors have been identified that work to govern *C. difficile* toxin expression (Martin-Verstraete et al., 2016). The uniting feature of many of these regulatory mechanisms is their connection with nutrient availability (Bouillaut et al., 2015). It is well established that the nutritional state of *C. difficile* has a major effect on the regulation of toxin expression, as well as the expression of nutrient acquisition mechanisms. Several studies have demonstrated that sugars and peptides suppress *C. difficile* toxin expression through the activity of nutrient-responsive regulators, such as CcpA and CodY (Dupuy and Sonenshein, 1998; Dineen et al., 2007; Antunes et al., 2011). When peptides and simple carbohydrates are depleted, the repression of toxin and nutrient acquisition mechanisms by CodY and CcpA is alleviated, and *C. difficile* utilizes alternative nutrients to sustain growth, though the details of this process *in vivo* are limited.

One particularly abundant potential nutrient in the intestine is phosphatidylethanolamine, a ubiquitous component of cell membranes that is readily hydrolyzed into ethanolamine and glycerol (Proulx and Fung, 1969; Larson et al., 1983). Ethanolamine is a simple amino alcohol that can serve as both a carbon and nitrogen source. Ethanolamine utilization genes have been identified and characterized in several pathogenic species that can inhabit the mammalian intestinal tract, including *Salmonella enterica* serovar Typhimurium, *Escherichia coli, Enterococcus faecalis* and *Listeria monocytogenes* (Faust et al., 1990; Stojiljkovic et al., 1995; Price-Carter et al., 2001; Del Papa and Perego, 2008; Toledo-Arana et al., 2009; Kendall et al., 2012). Though the predicted 19 gene cluster for ethanolamine utilization in *C. difficile* was identified when the first genome sequence was revealed, the functions and roles of these genes have not been investigated (Sebaihia et al., 2006).

As a strictly intestinal pathogen, the ability to utilize ethanolamine in the host could provide a growth advantage to *C. difficile*. In the current study, we examined the impact of ethanolamine and the putative ethanolamine utilization gene cluster, on the growth of *C. difficile*. In addition, we investigated the effect of ethanolamine metabolism on virulence in an animal model of infection. Using null mutants in the *eutA* and *eutG* genes, we demonstrate that *C. difficile* can utilize ethanolamine as a primary nutrient source and show that the proposed *eut* gene cluster is required for ethanolamine catabolism. Further, we found that the ability to utilize ethanolamine has a significant impact on the timing and intensity of disease in the hamster model of disease, indicating that ethanolamine utilization plays an important role in *C. difficile* pathogenesis.

RESULTS

C. difficile metabolizes ethanolamine as a primary nutrient source

In order to determine if the predicted *C. difficile eut* genes can facilitate ethanolamine metabolism, we first examined the growth of epidemic and historical isolates of *C. difficile* (R20291 and 630Δ*erm* strains, respectively) when ethanolamine is a major nutrient source

present in the growth medium (Supplementary File S1). As shown in Figure 1, *C. difficile* strains 630Δ*erm* and R20291 grown in a minimal defined medium with only amino acids present as a carbon source were able to replicate, but the bacteria reached stationary phase at a relatively low cell density. The addition of either ethanolamine or glucose to the medium produced a biphasic growth curve and increased the final density of the bacterial cultures, as well as the time needed to achieve maximum cell density. Notably, the 630Δ*erm* strain grew faster and to higher cell density than the R20291 strain under all of the tested conditions (Figure 1 and S3). No apparent differences in cellular morphology were observed between strains grown in minimal medium or with the addition of ethanolamine (Figure S4). The similar slope of logarithmic growth in minimal medium with and without added carbon sources, followed by a protracted growth phase with the addition of either glucose or ethanolamine, suggests that *C. difficile* most efficiently utilizes amino acids for growth.

eut gene expression is induced by ethanolamine, but is repressed by glucose and decreases during stationary phase growth in the absence of ethanolamine

The *C. difficile* genes encoding the ethanolamine utilization pathway and microcompartment structural components were first identified in the genome of strain 630 (*CD1907–CD1925;* Figure 2) (Sebaihia et al., 2006; Pitts et al., 2012). Although the ethanolamine genes are located on a mobile genetic element, this region is highly conserved in *C. difficile* genomes (> 700 genomes at the time of publication), including strains of the epidemic 027 and 078 lineages. Similar to the *Enterococcus faecalis* ethanolamine cluster, the 19 genes of the *C. difficile* cluster include 9 enzymes that are involved in ethanolamine metabolism, 6 proteins that comprise the predicted ethanolamine microcompartment, a two-component regulatory system, a transporter, and 1 gene of unknown function (Del Papa and Perego, 2008). An additional MarR-family transcriptional regulator is encoded downstream of the *eut* gene cluster in most *C. difficile* genomes, but this gene is not present in strain 630 (Figure 2A). As the putative *eut* gene cluster was the most likely basis for ethanolamine metabolism, we examined the expression of the *eut* genes during growth with and without added ethanolamine. Expression of the predicted *eut* cluster genes (*CD1907–CD1925*) was induced in response to ethanolamine in the culture medium, and was most pronounced during stationary phase growth (Figure 2B). In addition, expression of the gene immediately upstream of *eutG, CD1906*, was marginally affected by ethanolamine (1.5-fold increase). Two other predicted ethanolamine-related genes located on different regions of the chromosome, *CD0742* and *CD3167*, were also examined, and no change in expression was observed for either gene.

The expression analysis of the *eut* cluster revealed two distinct patterns of induction for these genes that suggests two polycistronic units are generated upon ethanolamine induction: a *eutG-eutW* transcript and a *eutA-eutQ* transcript (Figure 2B). Using cDNA generated from ethanolamine-induced cultures, we evaluated the entire *eut* gene cluster by performing PCR with primers designed to amplify across adjacent open reading frames to determine which genes were transcribed within the same mRNA (Figure S5). The predicted amplification products were generated across each adjacent *eut* gene, with the exception of the *eutW-eutA* segment, which contains a predicted transcriptional terminator that was previously identified (Fox et al., 2009; Ramesh et al., 2012). Altogether, these data demonstrate that the *eut* gene

cluster is comprised of at least two polycistronic units, both of which are induced by ethanolamine.

In *E. faecalis, eut* gene transcription is subject to positive regulatory control by the EutV-EutW two-component system, which disrupts a series of transcriptional terminators in the *eut* operon and allows transcription to progress (Del Papa and Perego, 2008; Fox et al., 2009; Garsin, 2010). Similar to *E. faecalis*, we observed basal expression of the *eutG-eutQ* genes during logarithmic growth in sporulation medium, in the absence of ethanolamine (Figure 3; ***eutA* shown**) (Fox et al., 2009). But, as cultures transitioned to stationary phase in sporulation medium, expression of all *eut* genes sharply decreased if ethanolamine was not present in the medium (Figure 3, *eutA* shown). The drastic decline in *eut* gene expression indicates that transcription is repressed during stationary phase, which is consistent with the previous observation that SigF-dependent repression of *eut* expression occurs in early sporulation (Fimlaid et al., 2013; Saujet et al., 2013).

Similar to the results in sporulation medium, *eut* gene expression increased during log-phase growth in minimal medium containing EA (Figure S6A). Although *eut* genes were induced in strain 630Δ*erm* and the epidemic isolate, R20291, the relative increase in *eutA* and *eutG* expression was lower in the epidemic strain. The difference in EA-dependent growth and *eut* gene induction between the strains suggests that the EA-dependent induction of the *eut* pathway varies within the species. However, both strains demonstrated no change in *eut* gene expression in the presence of glucose and intermediate induction of *eut* genes when both glucose and EA were available (Figure S6). The partial induction of *eut* genes with glucose and EA present is indicative of incomplete catabolite repression of *eut* gene expression. No change in *tcdA* or *tcdB* expression was observed for either strain when EA, glucose or the combination of EA and glucose were present in the medium (Figure S6B). The predicted regulator downstream of the *eut* operon in R20291, CDR20291_1847, also did not demonstrate differential expression in the presence of EA or glucose (Figure S6C).

Effects of *eut* gene disruption on ethanolamine metabolism

To determine the contribution of the predicted *eut* operons on ethanolamine metabolism, we generated null mutations via Targetron-based disruption of the upstream most genes of each operon: *eutG*, an alcohol dehydrogenase, and *eutA*, an ammonia lyase reactivating factor (Figures S7 and S8)(Karberg et al., 2001; Chen et al., 2005; Liu et al., 2007; Moore and Escalante-Semerena, 2016). The resulting strains were then tested for their ability to utilize ethanolamine as a primary nutrient source, as previously described (Figure 4). The *eutG* mutant retained the ability to utilize ethanolamine as a nutrient source, as evidenced by the wild-type-like, biphasic curve profile observed during growth in ethanolamine. However, the *eutA* strain displayed a single exponential growth phase in minimal medium, with or without the addition of ethanolamine, presumably because it was unable to metabolize ethanolamine (Figure 4). Further supporting the minimal medium studies, we observed that the *eutA* mutant did not produce a drop in the pH of TY medium supplemented with ethanolamine after 24 h growth, in contrast to the parent strain (Table 1). Hence, *eutA* is required for ethanolamine utilization, but *eutG* is not. We also observed that the genes downstream of *eutA* were not induced in the *eutA* mutant during growth in ethanolamine, implicating a

promoter upstream of *eutA* in ethanolamine-dependent transcription of *eutA-eutQ* (not shown). Altogether, the data support that the *CD1907–CD1925 eut* gene cluster is the primary mechanism for ethanolamine utilization in *C. difficile*.

The products of the *eutG* operon are involved in multiple aspects of ethanolamine processing, including enzymatic functions (*eutG* and *eutP*), microcompartment structure (*eutS*) and transcriptional regulation (*eutV* and *eutW*). The absence of an ethanolamine phenotype in the *eutG* mutant raised the question of how disruption of *eutG* impacts transcription of the four downstream genes, and what the overall importance of these factors are in ethanolamine utilization. To answer these questions, we further examined the transcription of each gene in the *eutG* operon in the *eutG* null mutant. As shown in Figure 5, insertional disruption of *eutG* reduced *eutG* expression, relative to the parent strain. But, expression of *eutS, eutP, eutV* and *eutW* were still induced in the *eutG* mutant when ethanolamine was added to the medium, signifying that an additional, ethanolamine-inducible promoter element is present in the intergenic region between *eutG* and *eutS*. Thus, the *eutG* null mutant is deficient only for *eutG* expression, which has no apparent impact on the growth of *C. difficile* in ethanolamine (Figure 4).

An inability to utilize ethanolamine leads to increased virulence in the hamster model of infection

The regulation of *C. difficile* toxin expression is highly integrated with nutrient availability, alternative energy metabolism, and regulators of metabolic gene expression (Yamakawa et al., 1994; Dupuy and Sonenshein, 1998; Dineen et al., 2007; Karlsson et al., 2008; Dineen et al., 2010; Antunes et al., 2011; Antunes et al., 2012; Bouillaut et al., 2013; Edwards et al., 2014; Dubois et al., 2016; Nawrocki et al., 2016). Previous studies of *C. difficile* pathogenesis have demonstrated links between metabolism and virulence in animal models of disease, while ethanolamine metabolism is specifically associated with virulence in other enteric species (Joseph et al., 2006; Maadani et al., 2007; Thiennimitr et al., 2011; Kendall et al., 2012; Edwards et al., 2014; Girinathan et al., 2016; Kansau et al., 2016). To determine if ethanolamine utilization impacts virulence in *C. difficile* infections, we examined the effects of the *eutA* mutant in a hamster model of *C. difficile* infection (CDI). Syrian golden hamsters were infected with spores of either the 630Δ*erm* parent strain or the *eutA* mutant, as described in the Methods. As shown in Figure 6A, hamsters infected with the *eutA* mutant succumbed to infection in less time than hamsters infected with the parent strain, and the variation in time to morbidity was significantly lower in *eutA* infections (630Δ*erm*, 56.0 ± 39.6 h; *eutA*, 33.7 ± 4.3; $P \leq 0.01$, log rank test). Hamsters infected with the *eutA* mutant also lost weight more rapidly post-infection than 630Δ*erm*-infected animals, consistent with the rapid time to morbidity observed (data not shown). Although *eutA*-infected animals demonstrated symptoms and became moribund more quickly, there was no significant difference in the number of *C. difficile* CFU recovered post-mortem (Figure 6B). These results suggest that the ability to utilize ethanolamine is not necessary for growth of the bacteria *in vivo*, but ethanolamine metabolism does delay pathogenesis during *C. difficile* infection.

Ethanolamine and ethanolamine catabolism do not affect the expression of virulence factors, sporulation or germination *in vitro*

As mentioned, the virulence gene expression and ethanolamine utilization are correlated in other enteric pathogens, and there is evidence that ethanolamine can serve as a signal to induce pathogenesis in some species (Garsin, 2010; Garsin, 2012; Kendall et al., 2012). In view of the increased virulence observed with the *eutA* mutant, we investigated the effects of ethanolamine and the ability to utilize ethanolamine on genes associated with pathogenesis. Transcriptional analyses of the major toxins, *tcdA* and *tcdB*, revealed no change in toxin expression for *C. difficile* grown in ethanolamine in the *eutA* mutant or the parent strain *in vitro* (Figure 7A,B). Likewise, no difference in TcdA protein levels was observed for strains grown in TY medium (Figure S9). We also examined transcription of the major type IV pilin, *pilA1*, and the flagellar subunit, *fliC*, which are involved in swarming and swimming motility, respectively (Purcell et al., 2012; Purcell et al., 2016). *C. difficile* flagella and pilin are detected by the innate immune system and can elicit a response that may impact pathogen clearance or virulence (Pechine et al., 2005; Pechine et al., 2007; Yoshino et al., 2013; Maldarelli et al., 2014; Batah et al., 2016; Ghose et al., 2016; Pechine and Collignon, 2016). Additionally, a connection between ethanolamine and pilin expression has been reported in *Escherichia coli* O157:H7 (Gonyar and Kendall, 2014). Neither *pilA1* nor *fliC* expression were impacted by the presence or ability to catabolize ethanolamine (Figure 7C,D). These data indicate that ethanolamine itself does not induce these common virulence factors *in vitro* and that the inability to utilize ethanolamine has no direct impact on the expression of the examined virulence genes.

Nutrient deprivation and regulation of nutritional responses have also been connected to early entry into the sporulation pathway and increased sporulation frequency for *C. difficile* (Dineen et al., 2010; Saujet et al., 2011; Antunes et al., 2012; Edwards and McBride, 2014; Edwards et al., 2014; Nawrocki et al., 2016). To determine if ethanolamine or ethanolamine utilization influence sporulation, we assessed sporulation frequency and sporulation-specific gene expression in the *eutA* mutant and parent strain grown in sporulation medium, with and without ethanolamine. No significant differences were observed in spore formation, sporulation frequency, or transcription of early sporulation genes for the mutant or parent strain grown in 15 mM ethanolamine (Figure S10). Increasing the concentration of ethanolamine to 30 mM also had no effect on sporulation outcomes (data not shown). Moreover, the *eutA* and *eutG* mutant spores had no observable germination defect *in vitro* (Figure S11). Altogether, these results suggest that ethanolamine does not feed into the nutritional regulatory pathways that influence sporulation in *C. difficile*.

DISCUSSION

Ethanolamine is an abundant membrane-derived compound present in the mammalian intestinal tract (Dowhan, 1997; Vance, 2008). Ethanolamine catabolism provides niche-specific growth advantages to select enteric bacteria, providing these species with an additional source of carbon and nitrogen, as well as extra energy generating potential in the intestinal environment. The ability to utilize ethanolamine has been shown to provide a nutritional growth advantage to other enteric pathogens, and in some cases, ethanolamine

amplifies pathogenic phenotypes by inducing the expression of virulence genes (Joseph et al., 2006; Del Papa and Perego, 2008; Srikumar and Fuchs, 2011; Kendall et al., 2012; Luzader et al., 2013; Anderson et al., 2015). Prior analyses of *C. difficile* gene expression during animal infections indicated that the ethanolamine utilization gene cluster is induced *in vivo*, but the effects of ethanolamine on growth and virulence were not known (Janoir et al., 2013). In the current work, we demonstrate that the predicted ethanolamine utilization gene cluster is necessary for ethanolamine utilization and this ability has a significant impact on the virulence of *C. difficile* in an animal model of infection.

As anticipated from the identification of the *eut* gene homologs on the chromosome and previous assessments of *in vivo* transcription and metabolic phenotyping, we demonstrated that *C. difficile* can utilize ethanolamine as a primary nutrient source (Sebaihia et al., 2006; Janoir et al., 2013; Scaria et al., 2014; Theriot and Young, 2014). The addition of ethanolamine to minimal medium supported additional growth and increased cell density, indicating that ethanolamine is catabolized (Figure 1). The expression of *eut* genes when glucose is present also suggests that *eut* gene expression can overcome catabolite repression. We also observed that *C. difficile* grew surprisingly well in base minimal medium with only amino acids as the primary nutrient source. This rapid, peptide-fueled growth was followed by a more protracted growth phase when glucose or ethanolamine were supplemented in the medium, suggesting that *C. difficile* preferentially catabolizes amino acids over sugars and ethanolamine. If *C. difficile* also prefers to metabolize amino acids over other carbon sources *in vivo*, the abundant peptide sources in the intestine could promote the rapid expansion of the population in the intestine (Smith and Macfarlane, 1998). Once the bulk of intestinal peptides are limiting, this dramatic population growth would presumably give way to a slower growth phase with a large population of bacteria to support, and less desired nutrient sources available. Unfortunately, it is difficult to definitively verify whether amino acids are the preferred nutrient source because *C. difficile* is auxotrophic for many amino acids and therefore, cannot grow without amino acid supplementation (Karasawa et al., 1995). But, it is clear that *C. difficile* encodes a remarkable repertoire of metabolic capabilities and can readily utilize other intestinal metabolites to generate energy, including a variety of carbohydrates (glucose, lactose, fructose, succinate, sucrose, lactose, trehalose, mannose, cellobiose, galactitol, tagatose, raffinose, stachyose, sorbitol, *N*-acetylglucosamine and sialic acid), peptides and amino acids via Stickland fermentation, and may even be capable of generating energy by fixation of CO_2 (Wilson and Perini, 1988; Karlsson et al., 2000; Jackson et al., 2006; Antunes et al., 2012; Bouillaut et al., 2013; Kopke et al., 2013; Ferreyra et al., 2014; Larocque et al., 2014; Theriot et al., 2014; Theriot and Young, 2015; Kansau et al., 2016).

Despite the large variety of energy sources that *C. difficile* can utilize, the importance of individual nutrient sources during infection is not well understood. Based on data from other enteric pathogens, we hypothesized that ethanolamine metabolism would be important for the growth of *C. difficile in vivo* and therefore, the ethanolamine mutant would be less fit for growth in the host than the parent strain (Stojiljkovic et al., 1995; Joseph et al., 2006; Maadani et al., 2007; Luzader et al., 2013; Anderson et al., 2015). Instead, the *eutA* mutant readily colonized hamsters, achieved equivalent cell densities, and caused more rapid morbidity than animals infected with the parent strain, 630Δ*erm*. These findings suggested

that ethanolamine utilization by *C. difficile* might delay the onset of virulence by postponing toxin expression, which is the main driver of symptoms and morbidity. Given the established links between nutrient availability and toxin expression in *C. difficile*, we further examined this phenomenon *in vitro* by assessing toxin gene transcription when ethanolamine was added to the growth medium (Figure 7). We observed no change in *tcdA* or *tcdB* transcription or protein production, suggesting that unlike other nutrients, there is no clear link between ethanolamine utilization and the regulation of toxin expression. In addition, ethanolamine supplementation did not impact sporulation frequency or motility gene regulation, as other nutrient sources do (Antunes et al., 2011; Antunes et al., 2012; El Meouche et al., 2013; McKee et al., 2013; Edwards et al., 2014; Edwards et al., 2016a; Nawrocki et al., 2016). The lack of ethanolamine influence on both sporulation and toxin expression strongly suggest that the major global nutritional regulators of sporulation, CodY and CcpA, do not respond directly or indirectly to ethanolamine. The increased virulence of the *eutA* mutant may be due to an overall lower nutrient availability *in vivo*, leading to earlier activation of toxin gene expression and virulence, but more work is needed to understand how ethanolamine specifically impacts *C. difficile* in the host.

It was anticipated that *eutA* and the downstream *eut* gene products would be required for ethanolamine metabolism, which was validated by growth assessments with ethanolamine (Figure 4). Less evident was the dispensability of EutG, which was not needed for the growth of *C. difficile* in ethanolamine. EutG is a predicted alcohol dehydrogenase that is involved in the enzymatic conversion of acetaldehyde to ethanol and is important for growth in ethanolamine for other species (Stojiljkovic et al., 1995). The acetaldehyde generated by the initial steps of ethanolamine metabolism is highly toxic to cells and must be detoxified, though the alternative pathway involving the EutE aldehyde dehydrogenase and the EutD phosphotransacetylase is still available in the *eutG* mutant for acetaldehyde disposal. The EutE-EutD path generates acetylphosphate, which could then be used to generate acetate, or shunted to either the TCA cycle or biosynthetic pathways (Stojiljkovic et al., 1995; Brinsmade et al., 2005; Garsin, 2010). Additionally, *C. difficile* strain 630 encodes another five predicted alcohol dehydrogenases that could potentially compensate for the loss of EutG: *CD0274, CD0334, CD2966, CD3006* and *CD3105*. However, the expression and functions of these factors in ethanolamine metabolism have not been investigated.

As observed in other species that encode extensive ethanolamine utilization mechanisms, the entire *C. difficile eut* gene cluster is induced when ethanolamine is present (Del Papa and Perego, 2008; Garsin, 2010; Anderson et al., 2015). *eut* gene induction in *C. difficile* is predicted to be controlled by the EutV-EutW two-component system, which was characterized previously in *E. faecalis* (Del Papa and Perego, 2008; Fox et al., 2009). In *E. faecalis*, EutW acts as the ethanolamine sensor histidine kinase that acts on the RNA-binding response regulator, EutV (Fox et al., 2009). Many Gram-negative species encode a positive regulator, EutR, an AraC-like DNA-binding protein that is needed for activation of *eut* gene expression (Tsoy et al., 2009). Although *C. difficile* encodes *eutV-eutW* and not the prototype Gram-negative EutR regulator, most *C. difficile* strains do encode a MarR-family regulator downstream from the *eut* gene cluster (CDR20291_1847 in strain R20291; Figure 2A). However, this MarR-family regulator is not present in the 630 genome. No changes in expression of this regulator were observed in the R20291 strain under any of the conditions

tested (Figure 6C). Further studies would be needed to determine if this putative regulator contributes to the differences in ethanolamine-dependent growth and gene expression observed in these strains.

The data also demonstrated that the *eut* genes were constitutively expressed at low levels in MMM during logarithmic phase, and subsequently repressed as cells entered stationary phase growth (Figure 3). This repression is consistent with the previous observation that the early sporulation sigma factor, SigF, represses *eut* gene expression in *C. difficile* (Saujet et al., 2013). Since SigF is a transcriptional activator, SigF-dependent repression of the *eut* genes is likely indirect. This stationary phase repression was overcome when ethanolamine was present (Figure 3), but no ethanolamine-dependent changes in spore formation or germination were observed (Figure S10 and S11). Stationary phase repression of ethanolamine genes has also been observed in *E. faecalis*, wherein the FsrABC quorum sensing regulatory system represses *eut* expression in post-exponential phase cells (Bourgogne et al., 2006). Sequenced *C. difficile* genomes do not encode apparent FsrABC proteins, but similar Agr-like systems have been identified in some strains (Martin et al., 2013). However, examination of transcription in an *agrA* mutant of strain R20291 did not uncover an impact of the Agr system on *eut* gene expression (Martin et al., 2013).

These results demonstrate both the function of the ethanolamine gene cluster and the importance of ethanolamine utilization on pathogenesis in an animal model of infection. Complementation studies or in frame deletions of individual ethanolamine utilization genes and regulators could help to clarify the precise regulatory mechanisms and functions of these factors, which we were unable to attain. Further study is needed to determine the precise regulatory mechanisms that govern *eut* gene expression in *C. difficile*, in particular to understand what function, if any, the putative MarR-like regulator plays in this process. Moreover, understanding the roles of individual metabolites, such as ethanolamine, in CDI, could help inform ways to circumvent pathogenesis and potentially guide treatment strategies for the prevention of fulminant disease.

EXPERIMENTAL PROCEDURES

Bacterial strains and growth conditions

Table 2 provides a list of the strains and plasmids used in this study. *C. difficile* strains were cultured in an anaerobic chamber (Coy Laboratory Products) at 37°C with an atmosphere of 10% H_2, 5% CO_2, and 85% N_2, as previously described (Bouillaut et al., 2011; Edwards et al., 2013). *C. difficile* strains were routinely cultured in brain heart infusion-supplemented (BHIS) broth and agar plates (Smith et al., 1981) or TY medium (adjusted to pH 7.4 prior to autoclaving)(Garnier and Cole, 1986). Two to ten μg of thiamphenicol ml^{-1}, or 5 μg of erythromycin ml^{-1} (Sigma-Aldrich) was used to supplement BHIS medium, as needed. *Escherichia coli* strains were cultured at 37°C in LB medium supplemented with 20 μg chloramphenicol ml^{-1} and 100 μg ampicillin ml^{-1}. Following conjugations, 50 μg kanamycin ml^{-1} was used to counter-select against *E. coli* (Purcell et al., 2012). To induce the germination of *C. difficile* spores, BHIS medium was supplemented with 0.1% taurocholate (Sigma-Aldrich) (Sorg and Sonenshein, 2008). D-fructose (0.2%) was added to overnight cultures to prevent sporulation, as needed (Putnam et al., 2013). Minimal medium

growth curves were performed using a modified minimal medium (MMM) based on previously described complete defined media (Karlsson et al., 1999; Cartman et al., 2012). This modified minimal medium contained lower final concentrations of amino acids and D-glucose than that used by Cartman *et al*. (Supplementary File S1). The base salts and amino acids of the minimal medium were supplemented with 5 mM D-glucose and/or 15 mM ethanolamine hydrochloride or liquid ethanolamine (Sigma-Aldrich), as noted. Growth curves in modified minimal medium (MMM) were performed as follows: log-phase cultures were grown to an OD_{600} of approximately 0.6 and back-diluted 6-fold to an OD_{600} of 0.1; the resulting dilution (OD_{600} 0.1) was then used to inoculate minimal medium at a further 1:10 dilution (2.5 ml into 22.5 ml of MMM). A minimum of three biological replicates were performed for each growth curve shown. The pH of cultures and solutions was measured as previously described (Edwards et al., 2016b).

Cloning and strain construction

Oligonucleotides used in this study are listed in Table 3. Construction details of plasmids used in this study can be found in Supplementary File S2. 630 genomic sequence (NC_009089.1) was used for primer design and null mutations were generated in 630Δ*erm* using a Targetron-based intron, as previously described (McBride and Sonenshein, 2011a; Purcell et al., 2012). *C. difficile* colonies were screened by PCR to verify intron insertion into the target gene. *C. difficile* DNA was isolated as described previously (Harju et al., 2004; Edwards et al., 2016a). Plasmids and cloned sequences were verified by standard sequencing (Eurofins MWG Operon). Conjugations of pMC263 and pMC266 into *C. difficile* strain 630Δ*erm* were performed as previously described (McBride and Sonenshein, 2011a). Given the very large *eut* genomic cluster (~17 kB), standard complementation of the Targetron-based mutant was unattainable in our hands. In lieu of complementation, whole-genome resequencing of the *eutA* mutant was performed to verify that the *eutA* phenotype was a direct result of the insertional mutation, and not unintended second-site mutations (detailed below).

Single-nucleotide polymorphisms (SNP) analysis

MC394 (*eutA::ermB*) and its parent strain, 630Δ*erm*, underwent SNP analysis to determine if any changes occurred in the *eutA* mutant other than the intended insertional disruption. Sample preparation and analyses were performed by the Yerkes Nonhuman Primate Genomics Core (Emory University). Libraries were generated from genomic DNA using the Illumina NexteraXT DNA kit, and dual barcoding and sequencing primers were used according to the manufacturer protocol. Libraries were validated by microelectrophoresis on an Agilent 2100 Bioanalyzer, quantified, pooled, and clustered on an Illumina miSeq V3 flowcell. The clustered flowcell was sequenced on an Illumina miSeq in 275-base paired-read reactions. Per sample reads were mapped to the *C. difficile* 630 reference genome (GenBank no. AM180355). CLC Genomics Workbench v9.0 was used for all variant analysis, as previously described (Childress et al., 2016). No nucleotide changes were observed between the mutant and parent strain genomes.

RNA isolation and quantitative reverse transcription PCR analysis (qRT-PCR)

qRT-PCR was performed as described previously with minor modifications (Edwards et al., 2014). *C. difficile* cultures were started in BHIS broth supplemented with 0.1% taurocholate and 0.2% fructose until they reached mid-logarithmic growth (OD_{600} of ~0.5). Cultures were then diluted 1:10 into 70:30 broth (70% SMC, 30% BHIS medium)(Putnam et al., 2013), with and without the addition of 15 mM ethanolamine hydrochloride (Sigma-Aldrich). Samples for RNA were collected at logarithmic growth (OD_{600} of ~0.5), mid-stationary phase (two hours after reaching an OD_{600} of ~1.0, T_2), and at late stationary phase (four hours after reaching an OD_{600} of ~1.0, T_4). Samples for RNA isolation were diluted in 1:1 acetone-ethanol and stored at −80°C. RNA isolation was performed as previously described (Dineen et al., 2010; McBride and Sonenshein, 2011a). Samples were treated with the Ambion DNAse Turbo Kit to remove contaminating genomic DNA, and cDNA synthesis was performed using a Bioline Tetro cDNA synthesis kit. qRT-PCR was performed with 50 ng of cDNA as template, using the Bioline Sensi-Fast SYBR and Fluroescein kit on a Roche LightCycler 96. qRT-PCR reactions were performed in technical triplicates and reactions containing no reverse transcriptase were included as negative controls. The PrimerQuest tool provided by Integrated DNA Technologies was used to generate qRT-PCR primers. The primer efficiencies for each primer set were determined using genomic DNA standards. qRT-PCR results were calculated by the comparative cycle threshold method (Schmittgen and Livak, 2008), with the expression of the amplified transcript being normalized to the internal control transcript, *rpoC*. A minimum of three biological replicates were performed and analyzed for each experimental set.

Hamster studies

Hamster studies were conducted as previously described with minor modifications (Woods et al., 2016). Male and female Syrian golden hamsters (*Mesocricetus auratus*) weighing between 70 to 110 grams were purchased from Charles River Laboratories. Hamsters were kept in an animal biosafety level 2 room within the Emory University Division of Animal Resources. Hamsters were housed individually with sterile rodent pellets and sterile water provided *ad libitum*. Hamsters were orally gavaged with clindamycin (30 mg/kg) to induce susceptibility to *C. difficile* seven days prior to inoculation (Day −7). Hamsters were inoculated by oral gavage with 5000 spores of 630Δ*erm* or MC394 (*eutA*::*ermB*) (Day 0). Hamsters treated with clindamycin, but not inoculated with *C. difficile* spores, served as negative controls. Spores were prepared as previously described (Edwards et al., 2014; Edwards and McBride, 2016; Woods et al., 2016). Following inoculation, hamsters were monitored for signs of disease, such as diarrhea or wet tail, weight loss, and lethargy. Hamsters were weighed and fecal pellets were collected once daily, if possible. Hamsters were considered moribund if they lost ≥ 15% of their body weight and/or exhibited severe disease symptoms. Hamsters meeting these criteria were euthanized in accordance with the American Veterinary Medical Association guidelines. Cecal contents were collected from animals post-mortem. Fecal and cecal contents were diluted in 1× PBS and plated onto taurocholate cycloserine cefoxitin fructose agar (TCCFA) plates to determine the number of *C. difficile* CFU (George et al., 1979; Wilson et al., 1981). Inoculated TCCFA plates were incubated anaerobically for 48 hours prior to CFU enumeration. Cecal content enumerations were analyzed using the Student's two-tailed *t* test and animal survival data were analyzed

using the log rank test. Three independent hamster experiments were conducted with cohorts of 5 to 6 hamsters per *C. difficile* strain; a total of 17 hamsters per strain were used.

Western blots and pH assessment

C. difficile strains were grown in BHIS medium containing 0.2% fructose and 0.1% taurocholate, as previously described. Cultures were diluted into BHIS medium and grown OD_{600} of ~0.5, then diluted 1:10 into TY medium with or without 15 mM ethanolamine, and grown for 24 h at 37°C. Cells were harvested by centrifugation, resuspended in SDS-PAGE loading buffer (without dye) and mechanically disrupted as previously described (Edwards et al., 2016a; Nawrocki et al., 2016). The pH of the cultures were also measured at the time of harvest, as previously described (Edwards et al., 2016b). Protein concentrations were assessed using a micro BCA assay (Thermo Scientific) and 8 μg of whole cell protein loaded onto a 12% polyacrylamide gel. Proteins were subsequently transferred from the SDS-PAGE gel onto nitrocellulose membranes (0.45 μM; Bio-Rad), and probed with mouse anti-TcdA antibody (Novus Biologicals). Membranes were then washed and probed with goat anti-mouse secondary Alexa Fluor 488 antibody (Life Technologies). Imaging and densitometry analyses were performed using a Bio-Rad ChemiDoc MP and Image Lab Software (Bio-Rad). Three biological replicates were analyzed for each strain and condition. Statistical analyses of the data were performed using a one-way ANOVA.

Phase contrast microscopy and direct count sporulation frequency

Samples for phase contrast microscopy were prepared as previously described (Edwards et al., 2014; Edwards and McBride, 2017). Briefly, samples were taken from 70:30 agar plates, resuspended in BHIS broth, and pipetted on to a 0.7% agarose pad on a glass slide. Micrographs were taken with a DS-Fi2 camera on a Nikon Eclipse Ci-L microscope with an X100 Ph3 oil-immersion objective. Direct count sporulation frequency was performed as previously described (Edwards et al., 2016a; Edwards and McBride, 2017). A minimum of 1000 cells were counted per strain and condition. Sporulation frequency was calculated by dividing the number of spores by the total number of cells present (spores and vegetative cells). MC310 (*spo0A::ermB*), a sporulation-defective mutant, was used as a negative control (Edwards et al., 2014). The mean sporulation frequencies and standard deviations were calculated from four independent experiments. Phase contrast sporulation frequency data were analyzed using a two-way repeated measures ANOVA.

Germination assays

C. difficile strains were grown on 70:30 sporulation agar and spores purified for germination studies as previously described, with some modifications (Nawrocki et al., 2016). Cultures on sporulation agar were removed from the anaerobic chamber after a minimum of 48 h of anaerobic growth and kept outside of the chamber in atmospheric oxygen overnight. Spore cultures were then scraped from the plates, resuspended in water, and frozen briefly at −80°C. After thawing, spore suspensions were centrifuged for 15 min at ~3200 × g in a swing bucket rotor, and the supernatant discarded. Spore pellets were then resuspended in 1 ml of a 1× PBS + 1% BSA solution, applied to a 12 ml 50% sucrose bed volume, and centrifuged at ~3200 × g for 20 min. The supernatant was then decanted and the spores were checked by phase-contrast microscopy for purity. Sucrose gradients were repeated until the

preparations reached a purity of greater than 95%. Spore pellets were then washed three times with 1× PBS + 1% BSA and resuspended to an OD_{600} = 3.0. Germination assays were carried out as previously described (Sorg and Sonenshein, 2008, 2009).

Accession numbers

C. difficile strain 630, GenBank accession NC_009089.1; strain R20291, GenBank accession NC_0133161.1.

Statistical analysis

Statistical analyses were performed using Excel and GraphPad Prism version 7.0 for Windows.

Supplementary Material

Refer to Web version on PubMed Central for supplementary material.

Acknowledgments

We thank members of the McBride lab, Charles Moran, Joanna Goldberg, David Weiss, and Philip Rather for their helpful suggestions and discussions during the course of this work.

FUNDING INFORMATION

This research was supported by the U.S. National Institutes of Health through research grants DK087763, DK101870, AI109526 and AI116933 to S.M.M., and T32 AI106699 to K.L.N. The content of this manuscript is solely the responsibility of the authors and does not necessarily reflect the official views of the National Institutes of Health.

References

Anderson CJ, Clark DE, Adli M, Kendall MM. Ethanolamine signaling promotes *Salmonella* niche recognition and adaptation during infection. PLoS Pathog. 2015; 11:e1005278. [PubMed: 26565973]

Antunes A, Martin-Verstraete I, Dupuy B. CcpA-mediated repression of *Clostridium difficile* toxin gene expression. Mol Microbiol. 2011; 79:882–899. [PubMed: 21299645]

Antunes A, Camiade E, Monot M, Courtois E, Barbut F, Sernova NV, et al. Global transcriptional control by glucose and carbon regulator CcpA in *Clostridium difficile*. Nucleic Acids Res. 2012; 40:10701–10718. [PubMed: 22989714]

Batah J, Deneve-Larrazet C, Jolivot PA, Kuehne S, Collignon A, Marvaud JC, Kansau I. *Clostridium difficile* flagella predominantly activate TLR5-linked NF-kappaB pathway in epithelial cells. Anaerobe. 2016; 38:116–124. [PubMed: 26790921]

Bouillaut L, McBride SM, Sorg JA. Genetic manipulation of *Clostridium difficile*. Curr Protoc Microbiol. 2011; Chapter 9(Unit 9A 2)

Bouillaut L, Self WT, Sonenshein AL. Proline-dependent regulation of *Clostridium difficile* Stickland metabolism. J Bacteriol. 2013; 195:844–854. [PubMed: 23222730]

Bouillaut L, Dubois T, Sonenshein AL, Dupuy B. Integration of metabolism and virulence in *Clostridium difficile*. Res Microbiol. 2015; 166:375–383. [PubMed: 25445566]

Bourgogne A, Hilsenbeck SG, Dunny GM, Murray BE. Comparison of OG1RF and an isogenic *fsrB* deletion mutant by transcriptional analysis: the Fsr system of *Enterococcus faecalis* is more than the activator of gelatinase and serine protease. J Bacteriol. 2006; 188:2875–2884. [PubMed: 16585749]

Brinsmade SR, Paldon T, Escalante-Semerena JC. Minimal functions and physiological conditions required for growth of *Salmonella enterica* on ethanolamine in the absence of the metabolosome. J Bacteriol. 2005; 187:8039–8046. [PubMed: 16291677]

Cartman ST, Kelly ML, Heeg D, Heap JT, Minton NP. Precise manipulation of the *Clostridium difficile* chromosome reveals a lack of association between the *tcdC* genotype and toxin production. Appl Environ Microbiol. 2012; 78:4683–4690. [PubMed: 22522680]

Chen Y, McClane BA, Fisher DJ, Rood JI, Gupta P. Construction of an alpha toxin gene knockout mutant of *Clostridium perfringens* type A by use of a mobile group II intron. Appl Environ Microbiol. 2005; 71:7542–7547. [PubMed: 16269799]

Childress KO, Edwards AN, Nawrocki KL, Woods EC, Anderson SE, McBride SM. The phosphotransfer protein CD1492 represses sporulation initiation in *Clostridium difficile*. Infect Immun. 2016

Del Papa MF, Perego M. Ethanolamine activates a sensor histidine kinase regulating its utilization in *Enterococcus faecalis*. J Bacteriol. 2008; 190:7147–7156. [PubMed: 18776017]

Dineen SS, McBride SM, Sonenshein AL. Integration of metabolism and virulence by *Clostridium difficile* CodY. J Bacteriol. 2010; 192:5350–5362. [PubMed: 20709897]

Dineen SS, Villapakkam AC, Nordman JT, Sonenshein AL. Repression of *Clostridium difficile* toxin gene expression by CodY. Mol Microbiol. 2007; 66:206–219. [PubMed: 17725558]

Dowhan W. Molecular basis for membrane phospholipid diversity: why are there so many lipids? Annu Rev Biochem. 1997; 66:199–232. [PubMed: 9242906]

Dubois T, Dancer-Thibonnier M, Monot M, Hamiot A, Bouillaut L, Soutourina O, et al. Control of *Clostridium difficile* physiopathology in response to cysteine availability. Infect Immun. 2016; 84:2389–2405. [PubMed: 27297391]

Dupuy B, Sonenshein AL. Regulated transcription of *Clostridium difficile* toxin genes. Mol Microbiol. 1998; 27:107–120. [PubMed: 9466260]

Edwards AN, McBride SM. Initiation of sporulation in *Clostridium difficile*: a twist on the classic model. FEMS Microbiol Lett. 2014; 358:110–118. [PubMed: 24910370]

Edwards AN, McBride SM. Isolating and Purifying *Clostridium difficile* Spores. Methods Mol Biol. 2016; 1476:117–128. [PubMed: 27507337]

Edwards AN, McBride SM. Determination of the in vitro Sporulation Frequency of *Clostridium difficile*. Bio-protocol. 2017; 7:1–8.

Edwards AN, Suarez JM, McBride SM. Culturing and maintaining *Clostridium difficile* in an anaerobic environment. J Vis Exp. 2013:e50787. [PubMed: 24084491]

Edwards AN, Nawrocki KL, McBride SM. Conserved oligopeptide permeases modulate sporulation initiation in *Clostridium difficile*. Infect Immun. 2014; 82:4276–4291. [PubMed: 25069979]

Edwards AN, Tamayo R, McBride SM. A novel regulator controls *Clostridium difficile* sporulation, motility and toxin production. Mol Microbiol. 2016a; 100:954–971. [PubMed: 26915493]

Edwards AN, Karim ST, Pascual RA, Jowhar LM, Anderson SE, McBride SM. Chemical and Stress Resistances of *Clostridium difficile* Spores and Vegetative Cells. Front Microbiol. 2016b; 7:1698. [PubMed: 27833595]

El Meouche I, Peltier J, Monot M, Soutourina O, Pestel-Caron M, Dupuy B, Pons JL. Characterization of the SigD regulon of *C. difficile* and its positive control of toxin production through the regulation of *tcdR*. PLoS One. 2013; 8:e83748. [PubMed: 24358307]

Faust LR, Connor JA, Roof DM, Hoch JA, Babior BM. Cloning, sequencing, and expression of the genes encoding the adenosylcobalamin-dependent ethanolamine ammonia-lyase of *Salmonella* Typhimurium. J Biol Chem. 1990; 265:12462–12466. [PubMed: 2197274]

Ferreyra JA, Wu KJ, Hryckowian AJ, Bouley DM, Weimer BC, Sonnenburg JL. Gut microbiota-produced succinate promotes *C. difficile* infection after antibiotic treatment or motility disturbance. Cell Host Microbe. 2014; 16:770–777. [PubMed: 25498344]

Fimlaid KA, Bond JP, Schutz KC, Putnam EE, Leung JM, Lawley TD, Shen A. Global Analysis of the Sporulation Pathway of *Clostridium difficile*. PLoS Genet. 2013; 9:e1003660. [PubMed: 23950727]

Fox KA, Ramesh A, Stearns JE, Bourgogne A, Reyes-Jara A, Winkler WC, Garsin DA. Multiple posttranscriptional regulatory mechanisms partner to control ethanolamine utilization in *Enterococcus faecalis*. Proc Natl Acad Sci U S A. 2009; 106:4435–4440. [PubMed: 19246383]

Garnier T, Cole ST. Characterization of a bacteriocinogenic plasmid from *Clostridium perfringens* and molecular genetic analysis of the bacteriocin-encoding gene. J Bacteriol. 1986; 168:1189–1196. [PubMed: 2877971]

Garsin DA. Ethanolamine utilization in bacterial pathogens: roles and regulation. Nat Rev Micro. 2010; 8:290–295.

Garsin DA. Ethanolamine: a signal to commence a host-associated lifestyle? MBio. 2012; 3:e00172–00112. [PubMed: 22761393]

George WL, Sutter VL, Citron D, Finegold SM. Selective and differential medium for isolation of *Clostridium difficile*. J Clin Microbiol. 1979; 9:214–219. [PubMed: 429542]

Ghose C, Eugenis I, Sun X, Edwards AN, McBride SM, Pride DT, et al. Immunogenicity and protective efficacy of recombinant *Clostridium difficile* flagellar protein FliC. Emerg Microbes Infect. 2016; 5:e8. [PubMed: 26839147]

Girinathan BP, Braun S, Sirigireddy AR, Lopez JE, Govind R. Importance of Glutamate Dehydrogenase (GDH) in *Clostridium difficile* Colonization In Vivo. PLoS One. 2016; 11:e0160107. [PubMed: 27467167]

Gonyar LA, Kendall MM. Ethanolamine and choline promote expression of putative and characterized fimbriae in enterohemorrhagic *Escherichia coli* O157:H7. Infect Immun. 2014; 82:193–201. [PubMed: 24126525]

Harju S, Fedosyuk H, Peterson KR. Rapid isolation of yeast genomic DNA: Bust n' Grab. BMC Biotechnol. 2004; 4:8. [PubMed: 15102338]

Ho TD, Ellermeier CD. PrsW is required for colonization, resistance to antimicrobial peptides, and expression of extracytoplasmic function sigma factors in *Clostridium difficile*. Infect Immun. 2011; 79:3229–3238. [PubMed: 21628514]

Hussain HA, Roberts AP, Mullany P. Generation of an erythromycin-sensitive derivative of *Clostridium difficile* strain 630 (630Δerm) and demonstration that the conjugative transposon Tn*916*ΔE enters the genome of this strain at multiple sites. J Med Microbiol. 2005; 54:137–141. [PubMed: 15673506]

Jackson S, Calos M, Myers A, Self WT. Analysis of proline reduction in the nosocomial pathogen *Clostridium difficile*. J Bacteriol. 2006; 188:8487–8495. [PubMed: 17041035]

Janoir C, Deneve C, Bouttier S, Barbut F, Hoys S, Caleechum L, et al. Adaptive strategies and pathogenesis of *Clostridium difficile* from *in vivo* transcriptomics. Infect Immun. 2013; 81:3757–3769. [PubMed: 23897605]

Joseph B, Przybilla K, Stuhler C, Schauer K, Slaghuis J, Fuchs TM, Goebel W. Identification of *Listeria monocytogenes* genes contributing to intracellular replication by expression profiling and mutant screening. J Bacteriol. 2006; 188:556–568. [PubMed: 16385046]

Kansau I, Barketi-Klai A, Monot M, Hoys S, Dupuy B, Janoir C, Collignon A. Deciphering Adaptation Strategies of the Epidemic *Clostridium difficile* 027 Strain during Infection through In Vivo Transcriptional Analysis. PLoS One. 2016; 11:e0158204. [PubMed: 27351947]

Karasawa T, Ikoma S, Yamakawa K, Nakamura S. A defined growth medium for *Clostridium difficile*. Microbiology. 1995; 141:371–375. [PubMed: 7704267]

Karberg M, Guo H, Zhong J, Coon R, Perutka J, Lambowitz AM. Group II introns as controllable gene targeting vectors for genetic manipulation of bacteria. Nat Biotechnol. 2001; 19:1162–1167. [PubMed: 11731786]

Karlsson S, Burman LG, Akerlund T. Suppression of toxin production in *Clostridium difficile* VPI 10463 by amino acids. Microbiology. 1999; 145(Pt 7):1683–1693. [PubMed: 10439407]

Karlsson S, Burman LG, Akerlund T. Induction of toxins in *Clostridium difficile* is associated with dramatic changes of its metabolism. Microbiology. 2008; 154:3430–3436. [PubMed: 18957596]

Karlsson S, Lindberg A, Norin E, Burman LG, Akerlund T. Toxins, butyric acid, and other short-chain fatty acids are coordinately expressed and down-regulated by cysteine in Clostridium difficile. Infect Immun. 2000; 68:5881–5888. [PubMed: 10992498]

Kendall MM, Gruber CC, Parker CT, Sperandio V. Ethanolamine controls expression of genes encoding components involved in interkingdom signaling and virulence in enterohemorrhagic *Escherichia coli* O157:H7. MBio. 2012; 3

Kopke M, Straub M, Durre P. *Clostridium difficile* is an autotrophic bacterial pathogen. PLoS One. 2013; 8:e62157. [PubMed: 23626782]

Kuehne SA, Cartman ST, Heap JT, Kelly ML, Cockayne A, Minton NP. The role of toxin A and toxin B in *Clostridium difficile* infection. Nature. 2010; 467:711–713. [PubMed: 20844489]

Larocque M, Chenard T, Najmanovich R. A curated *C. difficile* strain 630 metabolic network: prediction of essential targets and inhibitors. BMC Syst Biol. 2014; 8:117. [PubMed: 25315994]

Larson TJ, Ehrmann M, Boos W. Periplasmic glycerophosphodiester phosphodiesterase of *Escherichia coli* a new enzyme of the *glp* regulon. J Biol Chem. 1983; 258:5428–5432. [PubMed: 6304089]

Liu Y, Leal NA, Sampson EM, Johnson CL, Havemann GD, Bobik TA. PduL is an evolutionarily distinct phosphotransacylase involved in B12-dependent 1,2-propanediol degradation by *Salmonella enterica* serovar typhimurium LT2. J Bacteriol. 2007; 189:1589–1596. [PubMed: 17158662]

Luzader DH, Clark DE, Gonyar LA, Kendall MM. EutR is a direct regulator of genes that contribute to metabolism and virulence in enterohemorrhagic *Escherichia coli* O157: H7. J Bacteriol. 2013; 195:4947–4953. [PubMed: 23995630]

Lyerly DM, Saum KE, MacDonald DK, Wilkins TD. Effects of *Clostridium difficile* toxins given intragastrically to animals. Infect Immun. 1985; 47:349–352. [PubMed: 3917975]

Lyras D, O'Connor JR, Howarth PM, Sambol SP, Carter GP, Phumoonna T, et al. Toxin B is essential for virulence of *Clostridium difficile*. Nature. 2009; 458:1176–1179. [PubMed: 19252482]

Maadani A, Fox KA, Mylonakis E, Garsin DA. *Enterococcus faecalis* mutations affecting virulence in the *Caenorhabditis elegans* model host. Infect Immun. 2007; 75:2634–2637. [PubMed: 17307944]

Maldarelli GA, De Masi L, Rosenvinge EC, Carter M, Donnenberg MS. Identification, immunogenicity, and cross-reactivity of type IV pilin and pilin-like proteins from *Clostridium difficile*. Pathog dis. 2014; 71:302–314. [PubMed: 24550179]

Martin MJ, Clare S, Goulding D, Faulds-Pain A, Barquist L, Browne HP. The agr locus regulates virulence and colonization genes in *Clostridium difficile* 027. J Bacteriol. 2013; 195:3672–3681. [PubMed: 23772065]

Martin-Verstraete I, Peltier J, Dupuy B. The regulatory networks that control *Clostridium difficile* toxin synthesis. Toxins (Basel). 2016; 8

McBride SM, Sonenshein AL. The *dlt* operon confers resistance to cationic antimicrobial peptides in *Clostridium difficile*. Microbiology. 2011a; 157:1457–1465. [PubMed: 21330441]

McBride SM, Sonenshein AL. Identification of a genetic locus responsible for antimicrobial peptide resistance in *Clostridium difficile*. Infect Immun. 2011b; 79:167–176. [PubMed: 20974818]

McKee RW, Mangalea MR, Purcell EB, Borchardt EK, Tamayo R. The second messenger cyclic Di-GMP regulates *Clostridium difficile* toxin production by controlling expression of *sigD*. J Bacteriol. 2013; 195:5174–5185. [PubMed: 24039264]

Moore TC, Escalante-Semerena JC. The EutQ and EutP proteins are novel acetate kinases involved in ethanolamine catabolism: physiological implications for the function of the ethanolamine metabolosome in *Salmonella enterica*. Mol Microbiol. 2016; 99:497–511. [PubMed: 26448059]

Nawrocki KL, Edwards AN, Daou N, Bouillaut L, McBride SM. CodY-dependent regulation of sporulation in *Clostridium difficile*. J Bacteriol. 2016; 198:2113–2130. [PubMed: 27246573]

Pechine S, Collignon A. Immune responses induced by *Clostridium difficile*. Anaerobe. 2016; 41:68–78. [PubMed: 27108093]

Pechine S, Gleizes A, Janoir C, Gorges-Kergot R, Barc MC, Delmee M, Collignon A. Immunological properties of surface proteins of *Clostridium difficile*. J Med Microbiol. 2005; 54:193–196. [PubMed: 15673516]

Pechine S, Janoir C, Boureau H, Gleizes A, Tsapis N, Hoys S, et al. Diminished intestinal colonization by *Clostridium difficile* and immune response in mice after mucosal immunization with surface proteins of *Clostridium difficile*. Vaccine. 2007; 25:3946–3954. [PubMed: 17433506]

Pitts AC, Tuck LR, Faulds-Pain A, Lewis RJ, Marles-Wright J. Structural insight into the *Clostridium difficile* ethanolamine utilisation microcompartment. PLoS One. 2012; 7:e48360. [PubMed: 23144756]

Price-Carter M, Tingey J, Bobik TA, Roth JR. The Alternative Electron Acceptor Tetrathionate Supports B12-Dependent Anaerobic Growth of *Salmonella enterica* Serovar Typhimurium on Ethanolamine or 1,2-Propanediol. J Bacteriol. 2001; 183:2463–2475. [PubMed: 11274105]

Proulx P, Fung CK. Metabolism of phosphoglycerides in E. coli. IV. The positional specificity and properties of phospholipase A. Can J Biochem. 1969; 47:1125–1128. [PubMed: 4903510]

Purcell EB, McKee RW, McBride SM, Waters CM, Tamayo R. Cyclic diguanylate inversely regulates motility and aggregation in *Clostridium difficile*. J Bacteriol. 2012; 194:3307–3316. [PubMed: 22522894]

Purcell EB, McKee RW, Bordeleau E, Burrus V, Tamayo R. Regulation of Type IV Pili Contributes to Surface Behaviors of Historical and Epidemic Strains of *Clostridium difficile*. J Bacteriol. 2016; 198:565–577. [PubMed: 26598364]

Putnam EE, Nock AM, Lawley TD, Shen A. SpoIVA and SipL are *Clostridium difficile* spore morphogenetic proteins. J Bacteriol. 2013; 195:1214–1225. [PubMed: 23292781]

Ramesh A, DebRoy S, Goodson JR, Fox KA, Faz H, Garsin DA, Winkler WC. The mechanism for RNA recognition by ANTAR regulators of gene expression. PLoS Genet. 2012; 8:e1002666. [PubMed: 22685413]

Saujet L, Monot M, Dupuy B, Soutourina O, Martin-Verstraete I. The key sigma factor of transition phase, SigH, controls sporulation, metabolism, and virulence factor expression in *Clostridium difficile*. J Bacteriol. 2011; 193:3186–3196. [PubMed: 21572003]

Saujet L, Pereira FC, Serrano M, Soutourina O, Monot M, Shelyakin PV, et al. Genome-Wide Analysis of Cell Type-Specific Gene Transcription during Spore Formation in *Clostridium difficile*. PLoS Genet. 2013; 9:e1003756. [PubMed: 24098137]

Scaria J, Chen JW, Useh N, He H, McDonough SP, Mao C, et al. Comparative nutritional and chemical phenome of *Clostridium difficile* isolates determined using phenotype microarrays. Int J Infect Dis. 2014; 27C:20–25.

Schmittgen TD, Livak KJ. Analyzing real-time PCR data by the comparative C(T) method. Nat Protoc. 2008; 3:1101–1108. [PubMed: 18546601]

Sebaihia M, Wren BW, Mullany P, Fairweather NF, Minton N, Stabler R, et al. The multidrug-resistant human pathogen *Clostridium difficile* has a highly mobile, mosaic genome. Nat Genet. 2006; 38:779–786. [PubMed: 16804543]

Smith CJ, Markowitz SM, Macrina FL. Transferable tetracycline resistance in *Clostridium difficile*. Antimicrob Agents Chemother. 1981; 19:997–1003. [PubMed: 7271279]

Smith EA, Macfarlane GT. Enumeration of amino acid fermenting bacteria in the human large intestine: effects of pH and starch on peptide metabolism and dissimilation of amino acids. FEMS Microbiol Ecol. 1998; 25:355–368.

Sorg JA, Sonenshein AL. Bile salts and glycine as cogerminants for *Clostridium difficile* spores. J Bacteriol. 2008; 190:2505–2512. [PubMed: 18245298]

Sorg JA, Sonenshein AL. Chenodeoxycholate is an inhibitor of *Clostridium difficile* spore germination. J Bacteriol. 2009; 191:1115–1117. [PubMed: 19060152]

Srikumar S, Fuchs TM. Ethanolamine utilization contributes to proliferation of *Salmonella enterica* serovar Typhimurium in food and in nematodes. Appl Environ Microbiol. 2011; 77:281–290. [PubMed: 21037291]

Stabler RA, He M, Dawson L, Martin M, Valiente E, Corton C, et al. Comparative genome and phenotypic analysis of *Clostridium difficile* 027 strains provides insight into the evolution of a hypervirulent bacterium. Genome Biol. 2009; 10:R102. [PubMed: 19781061]

Stojiljkovic I, Baumler AJ, Heffron F. Ethanolamine utilization in *Salmonella typhimurium*: nucleotide sequence, protein expression, and mutational analysis of the *cchA cchB eutE eutJ eutG eutH* gene cluster. J Bacteriol. 1995; 177:1357–1366. [PubMed: 7868611]

Theriot CM, Young VB. Microbial and metabolic interactions between the gastrointestinal tract and *Clostridium difficile* infection. Gut Microbes. 2014; 5:86–95. [PubMed: 24335555]

Theriot CM, Young VB. Interactions Between the Gastrointestinal Microbiome and *Clostridium difficile*. Annu Rev Microbiol. 2015; 69:445–461. [PubMed: 26488281]

Theriot CM, Koenigsknecht MJ, Carlson PE Jr, Hatton GE, Nelson AM, Li B, et al. Antibiotic-induced shifts in the mouse gut microbiome and metabolome increase susceptibility to *Clostridium difficile* infection. Nat Commun. 2014; 5:3114. [PubMed: 24445449]

Thiennimitr P, Winter SE, Winter MG, Xavier MN, Tolstikov V, Huseby DL, et al. Intestinal inflammation allows *Salmonella* to use ethanolamine to compete with the microbiota. Proc Natl Acad Sci U S A. 2011; 108:17480–17485. [PubMed: 21969563]

Thomas CM, Smith CA. Incompatibility group P plasmids: genetics, evolution, and use in genetic manipulation. Ann Rev Microbiol. 1987; 41:77–101. [PubMed: 3318684]

Toledo-Arana A, Dussurget O, Nikitas G, Sesto N, Guet-Revillet H, Balestrino D, et al. The *Listeria* transcriptional landscape from saprophytism to virulence. Nature. 2009; 459:950–956. [PubMed: 19448609]

Tsoy O, Ravcheev D, Mushegian A. Comparative genomics of ethanolamine utilization. J Bacteriol. 2009; 191:7157–7164. [PubMed: 19783625]

Vance JE. Phosphatidylserine and phosphatidylethanolamine in mammalian cells: two metabolically related aminophospholipids. J Lipid Res. 2008; 49:1377–1387. [PubMed: 18204094]

Wilson KH, Perini F. Role of competition for nutrients in suppression of *Clostridium difficile* by the colonic microflora. Infect Immun. 1988; 56:2610–2614. [PubMed: 3417352]

Wilson KH, Silva J, Fekety FR. Suppression of *Clostridium difficile* by normal hamster cecal flora and prevention of antibiotic-associated cecitis. Infect Immun. 1981; 34:626–628. [PubMed: 7309245]

Woods EC, Nawrocki KL, Suarez JM, McBride SM. The *Clostridium difficile* Dlt pathway is controlled by the ECF sigma factor, SigmaV, in response to lysozyme. Infect Immun. 2016

Yamakawa K, Kamiya S, Meng X, Karasawa T, Nakamura S. Toxin production by *Clostridium difficile* in a defined medium with limited amino acids. J Med Microbiol. 1994; 41:319–323. [PubMed: 7966203]

Yoshino Y, Kitazawa T, Ikeda M, Tatsuno K, Yanagimoto S, Okugawa S, et al. *Clostridium difficile* flagellin stimulates toll-like receptor 5, and toxin B promotes flagellin-induced chemokine production via TLR5. Life Sci. 2013; 92:211–217. [PubMed: 23261530]

Originality-Significance Statement

This work represents the first investigation of ethanolamine utilization in *C. difficile* and our data demonstrate that ethanolamine represents more than simply an alternative nutrient source for this important pathogen. These results represent a significant advance in understanding how nutrition impacts *C. difficile* virulence.

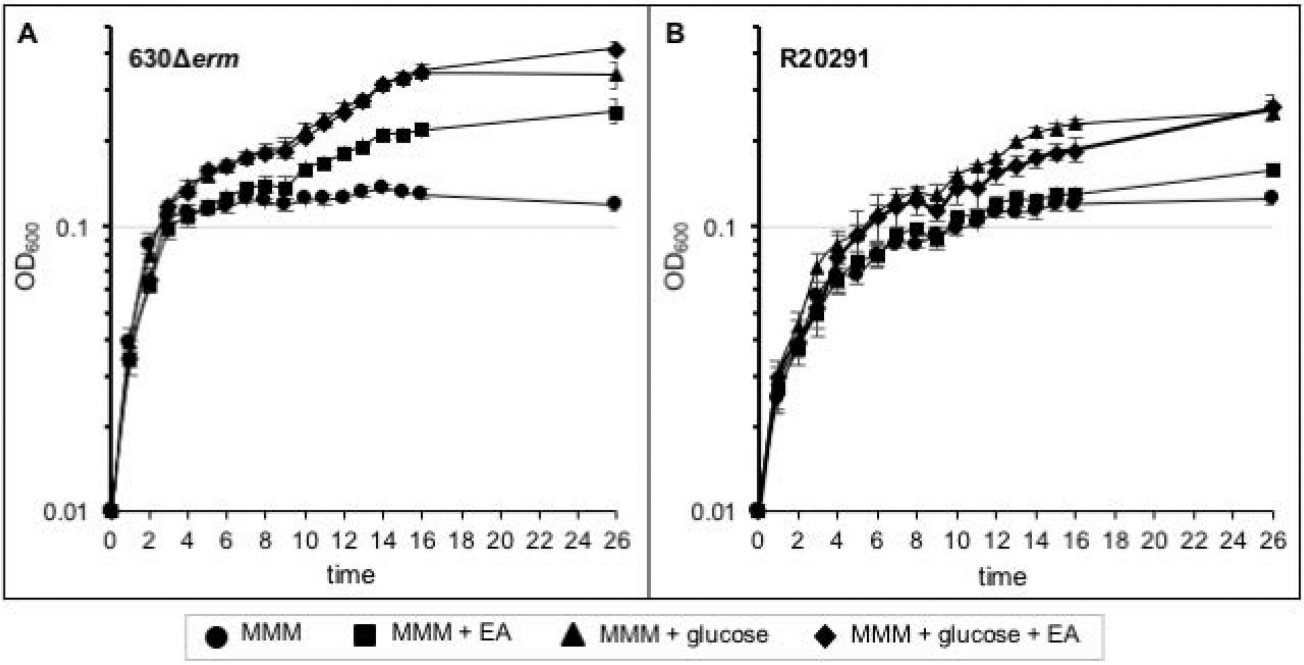

Figure 1. ***C. difficile*** **metabolizes ethanolamine as a primary nutrient source**

Growth curve of strain **A)** 630Δ*erm* or **B)** R20291 in modified minimal medium (MMM) or MMM supplemented with 15 mM ethanolamine (EA) and/or 5 mM D-glucose. The average of three independent biological replicates and standard deviations are shown.

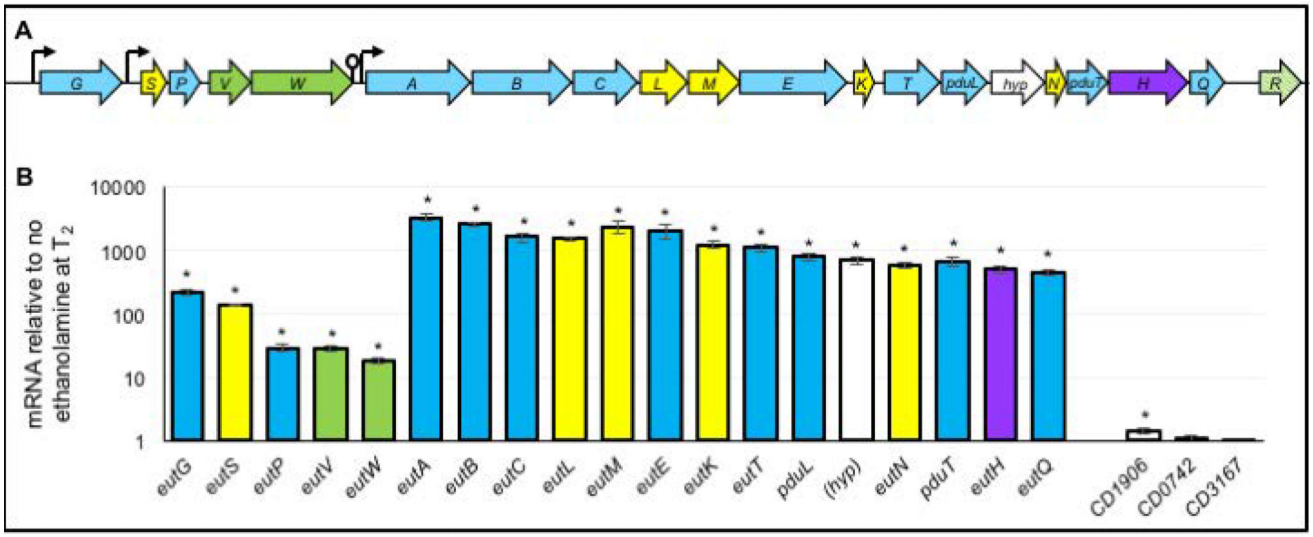

Figure 2. Expression of ethanolamine utilization genes in *C. difficile*

A) Ethanolamine utilization (*eut*) gene cluster in *C. difficile (eutG-eutQ)*. The *eut* gene cluster contains 19 predicted open reading frames (predicted functions listed in File S7). Genes in blue encode predicted metabolic enzymes, green encode regulatory factors, yellow are predicted microcompartment structural proteins, purple encode the putative transporter and white (*hyp*) is of unknown function. The putative factor downstream of *eutQ* (R, green stripes) is a MarR-family transcriptional regulator encoded in most sequenced *C. difficile* isolates downstream of *eutQ*, but is not found in strain 630. Suspected promoters and terminators are shown as arrows and lollipops, respectively. (B) qRT-PCR analysis of putative *eut* gene expression in strain 630Δ*erm* grown in 70:30 liquid medium with and without the addition of 15 mM ethanolamine (EA). Samples were harvested for RNA isolation two hours after the entry into stationary phase (T_2). The means and standard error of the means of three biological replicates are shown. *, $p \leq 0.05$ by Student's two-tailed *t*-test.

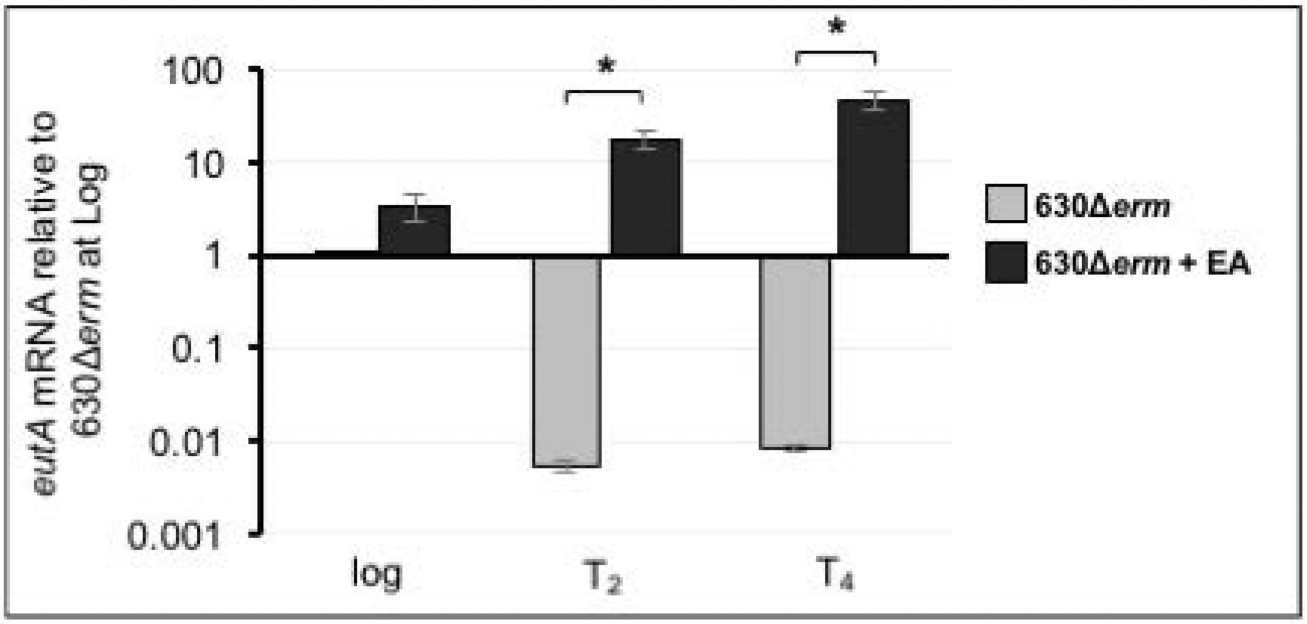

Figure 3. *eut* gene expression increases in response to ethanolamine, but expression is repressed during stationary phase if ethanolamine is absent

qRT-PCR analysis of *eutA* expression of 630Δ*erm* grown in 70:30 liquid medium with and without the addition of 15 mM ethanolamine (EA). Expression of *eutA* in 630Δ*erm* grown in medium with and without EA was compared at each timepoint using the Student's two-tailed *t*-test. The means and standard error of the means of three biological replicates are shown. * indicates $p \leq 0.05$.

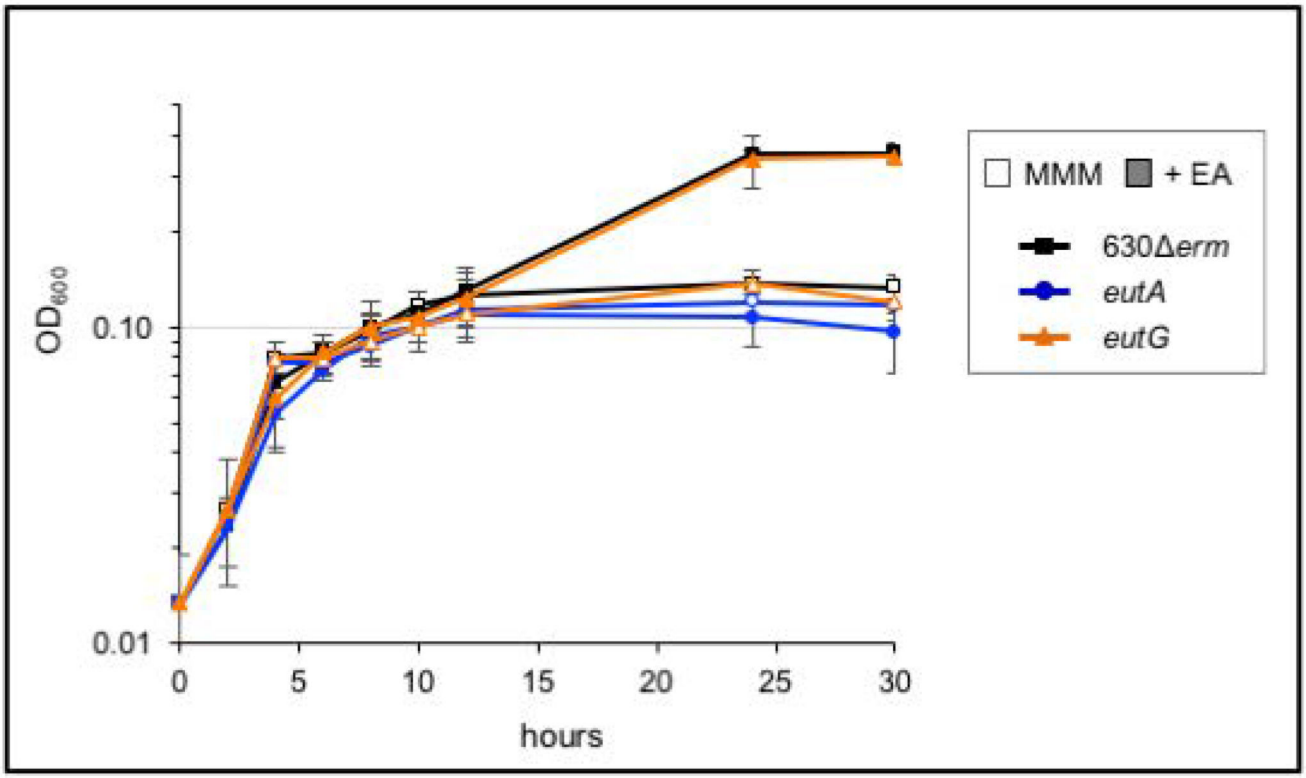

Figure 4. The *eutA* operon, and not the *eutG* transcriptional unit, is essential for ethanolamine metabolism in *C. difficile*

Growth curve with 630Δ*erm* (black squares), *eutA* (MC394; blue circles) and the *eutG* strain (MC346; orange triangles) grown in modified minimal medium (MMM; open symbols) and with the addition of 15 mM ethanolamine (EA; filled symbols). Averages and standard deviations of three independent experiments shown.

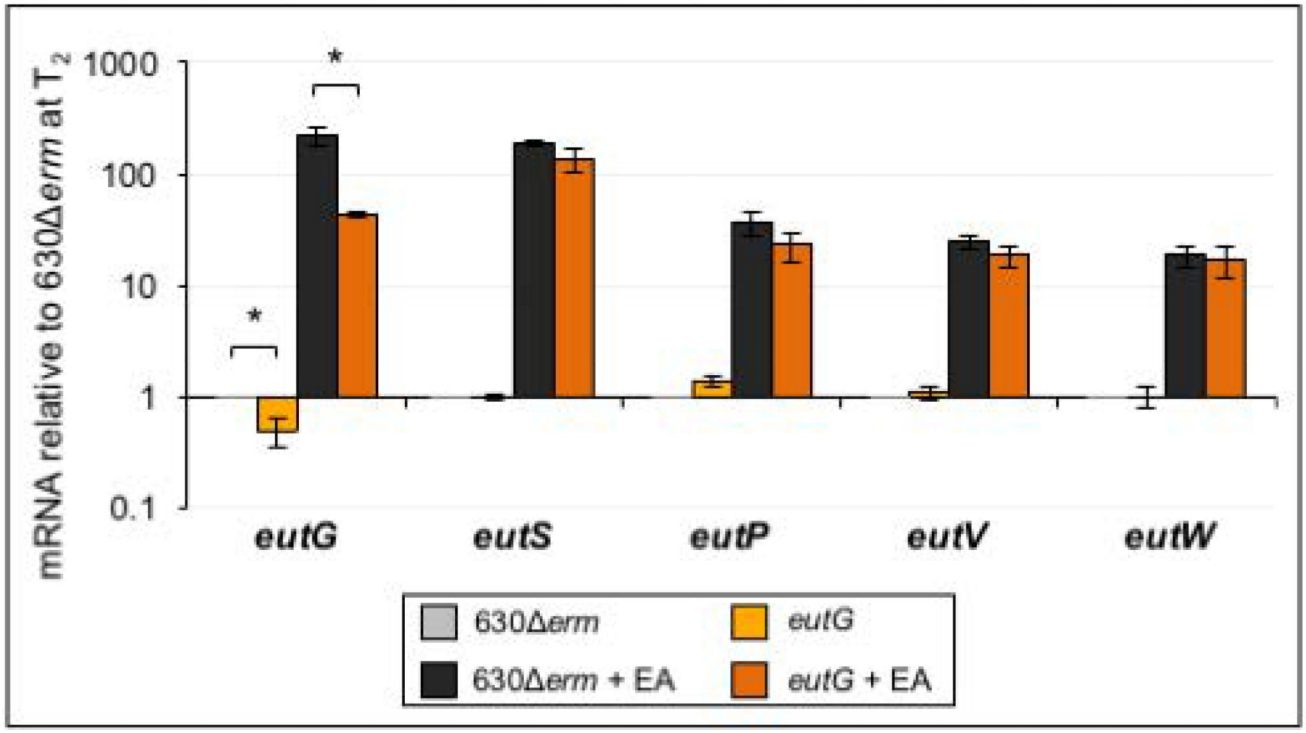

Figure 5. Insertional disruption of *eutG* does not affect transcription of downstream genes

qRT-PCR analysis of *eutG, eutS, eutP, eutV* and *eutW* expression in 630Δ*erm* and the *eutG* mutant (MC346) grown in 70:30 broth with and without the addition of 15 mM ethanolamine (EA). Samples for RNA isolation were collected two hours after the transition into stationary phase (T_2). The means and standard error of the means for three biological replicates are shown. Gene expression of 630Δ*erm* and the *eutG* mutant were compared for each condition using the Student's two-tailed *t*-test. * indicates $p \leq 0.05$.

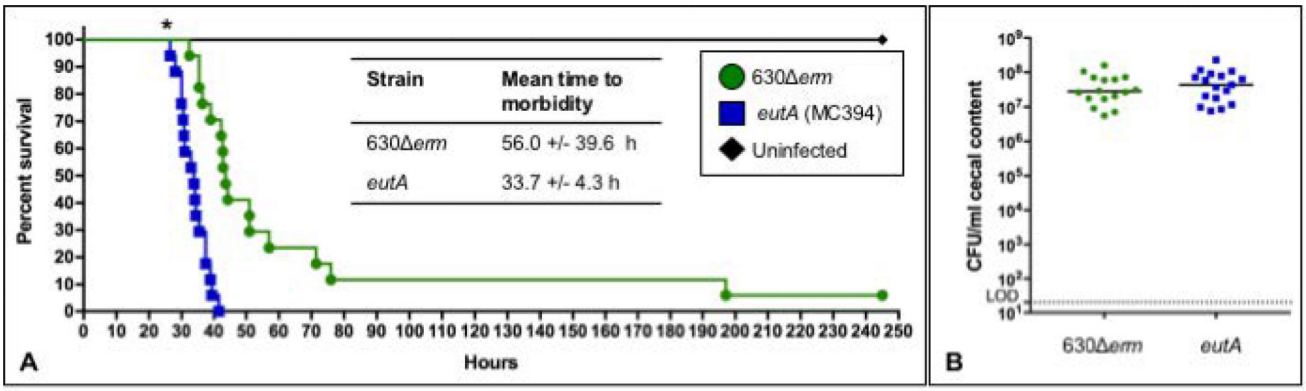

Figure 6. A *eutA* mutant is more virulent in the hamster model of CDI

A) Kaplan-Meier survival curve representing the results from three independent experiments of Syrian golden hamsters infected with *C. difficile* strain 630Δ*erm* (n=17) or the *eutA* mutant (MC394; n=17). The mean times to morbidity were 56 +/− 39.6 h for 630Δ*erm* and 33.7 +/− 4.3 h for the *eutA* mutant ($P \leq 0.01$, log rank test). **B)** Total CFU of *C. difficile* were enumerated from hamster cecal samples collected post-mortem. Solid lines represent the median CFU for each strain and the dotted line denotes the limit of detection (2×10^1 CFU ml^{-1}). CFU for the mutant and parent strains were compared using the Student's two-tailed *t* test (no statistically significant differences were observed).

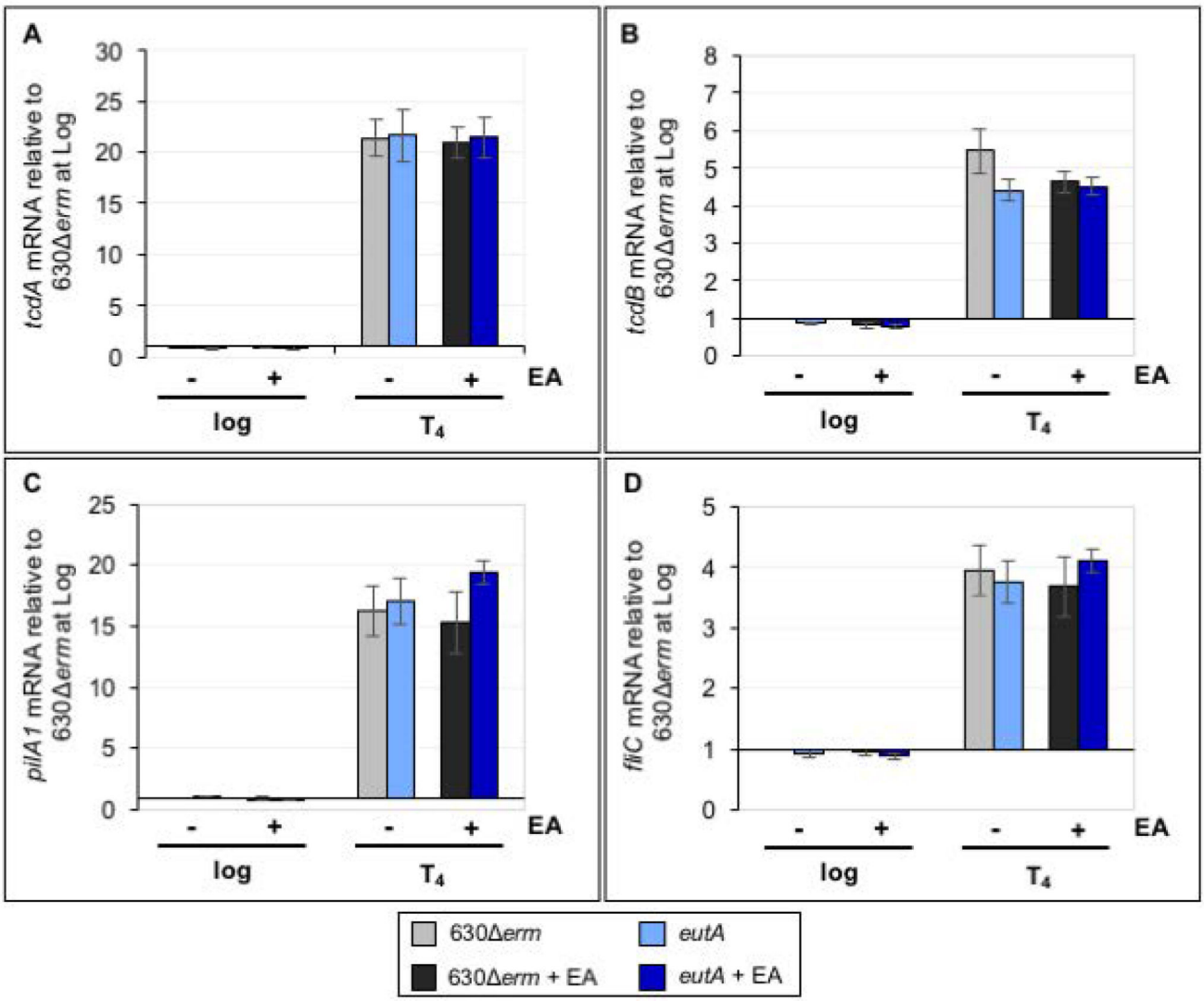

Figure 7. Ethanolamine metabolism does not impact expression of known virulence factors *in vitro*

qRT-PCR analysis of **A)** *tcdA*, **B)** *tcdB*, **C)** *pilA1* and **D)** *fliC* expression in 630Δ*erm* and the *eutA* mutant (MC394) grown in 70:30 broth with and without the addition of 15 mM EA. Samples for RNA isolation were collected during logarithmic growth (Log, OD_{600} of 0.5) and four hours after the transition into stationary phase (T4, late stationary). The means and standard error of the means of four biological replicates are shown. Gene expression of 630Δ*erm* and the *eutA* mutant were compared at each timepoint and condition using the Student's two-tailed *t*-test. * indicates $p \leq 0.05$ (no significant differences were observed).

Table 1

pH of *eut* cultures after 24h growth

Strain/condition	Final pH[a]
630Δ*erm* / TY	7.41 ± 0.17
630Δ*erm* / TY+EA 15 mM	7.23 ± 0.16
630Δ*erm* / TY+EA 30 mM	7.05 ± 0.14
630Δ*erm* / TY+EA 45 mM	6.89 ± 0.13
eutA / TY	7.37 ± 0.16
eutA / TY+EA 15 mM	7.32 ± 0.13
eutA / TY+EA 30 mM	**7.33 ± 0.13**
eutA / TY+EA 45 mM	**7.30 ± 0.12**
eutG / TY	7.30 ± 0.13
eutG / TY+EA 15 mM	7.20 ± 0.14
eutG / TY+EA 30 mM	7.06 ± 0.12
eutG / TY+EA 45 mM	6.91 ± 0.10

[a] mean pH of four biological replicates +/− standard deviation shown

[b] bold indicates statistically significant difference between the mutant and parent strain for a given condition ($p \leq 0.05$; ANOVA with Sidak's multiple-comparison test)

Table 2

Bacterial Strains and plasmids

Plasmid or Strain		Relevant genotype or features	Source, construction or reference
Strains			
E. coli			
	HB101	F$^-$ *mcrB mrr hsdS20*(r_B^- m_B^-) *recA13 leuB6 ara-14 proA2 lacY1 galK2 xyl-5 mtl-1 rpsL20*	B. Dupuy
	MC101	HB101 pRK24	B. Dupuy
	DH5α Max Efficiency	F$^-$ Φ80*lacZ*ΔM15 Δ(*lacZ*YA-*arg*F) U169 *rec*A1 *end*A1 *hsd*R17 (rk^-, mk^+) *pho*A *sup*E44 λ^- *thi*$^-$ 1 *gyr*A96 *rel*A1	Invitrogen
	MC341	HB101 pRK24 pMC263	This study
	MC344	HB101 pRK24 pMC266	This study
C. difficile			
	R20291	Clinical isolate; ribotype 027	(Stabler et al., 2009)
	630Δ*erm*	Erm^S derivative of strain 630	N. Minton (Hussain et al., 2005)
	MC310	630Δ*erm spo0A::ermB*	(Edwards et al., 2014)
	MC346	630Δ*erm eutG::ermB*	This study
	MC394	630Δ*erm eutA::ermB*	This study
Plasmids	pCE240	*C. difficile* Targetron construct based on pJIR750ai (group II intron, *ermB*::RAM *ltrA*) *catP*	C. Ellermeier (Ho and Ellermeier, 2011)
	pRK24	Tra^+, Mob^+; *bla, tet*	(Thomas and Smith, 1987)
	pCR2.1	*bla kan*	Invitrogen
	pMC123	*E. coli-C. difficile* shuttle vector; *bla, catP*	(McBride and Sonenshein, 2011b)
	pMC253	pCR2.1 Group II intron targeting region for *eutA*	This study
	pMC256	pCR2.1 Group II intron targeting region for *eutG*	This study
	pMC257	pCE240 Group II intron targeted to *eutA*	This study
	pMC260	pCE240 Group II intron targeted to *eutG*	This study
	pMC263	pMC123 Group II intron targeted to *eutA, ermB*::RAM *ltrA catP*	This study
	pMC266	pMC123 Group II intron targeted to *eutG, ermB*::RAM ltrA catP	This study

Table 3

Oligonucleotides

Primer	Sequence (5'→3')	Use/location[a]	Source or reference
EBS universal	5'-CGAAATTAGAAACTTGCGTTCAGTAAAC-3'	Targetron cloning	Sigma-Aldrich
oMC44	5'-CTAGCTGCTCCTATGTCTCACATC-3'	*rpoC* PCR (CD0067)	(McBride and Sonenshein, 2011a)
oMC45	5'-CCAGTCTCTCCTGGATCAACTA-3'	*rpoC* PCR (CD0067)	(McBride and Sonenshein, 2011a)
oMC112	5'-GGCAAATGTAAGATTTCGTACTCA-3'	*tcdB* PCR (CD0660)	(Edwards et al., 2014)
oMC113	5'-TCGACTACAGTATTCTCTGAC-3'	*tcdB* PCR (CD0660)	(Edwards et al., 2014)
oMC339	5'-GGGCAAATATACTTCCTCCTCCAT-3'	*sigE* PCR (CD2643)	(Edwards et al., 2014)
oMC340	5'-TGACTTTACACTTTCATCTGTTTCTAGC-3'	*sigE* PCR (CD2643)	(Edwards et al., 2014)
oMC547	5'-TGGATAGGTGGAGAAGTCAGT-3'	*tcdA* PCR (CD0663)	(Edwards et al., 2014)
oMC548	5'-GCTGTAATGCTTCAGTGGTAGA-3'	*tcdA* PCR (CD0663)	(Edwards et al., 2014)
oMC655	5'-GAAATAGTACCAGACCCACCAATA-3'	*eutG* PCR (CD1907)	This study
oMC656	5'-TATTGCAGAACCACCACCTAAT-3'	*eutG* PCR (CD1907)	This study
oMC657	5'-CTAAAGAAGATATACATACAGGAGCAGT-3'	*eutA* PCR (CD1912)	This study
oMC658	5'-TAAATCAGGTCCTGCTGTTGC-3'	*eutA* PCR (CD1912)	This study
oMC659	5'-ATCAGGAGATAAATTAGCAGGTCTT-3'	*eutB* PCR (CD1913)	This study
oMC660	5'-GCCACTGCAGGATTATTTCTTATATC-3'	*eutB* PCR (CD1913)	This study
oMC661	5'-GTTGATGATGAACCACTGTTAAGG-3'	*eutV* PCR (CD1910)	This study
oMC662	5'-TTCAACAGCTTCAAATCCATCAC-3'	*eutV* PCR (CD1910)	This study
oMC663	5'-TGTACTAAGTAAATTTGATGATGAAGCA-3'	*eutW* PCR (CD1911)	This study
oMC664	5'-TGACCAGTTTATATTCCTGTGTTAAAG-3'	*eutW* PCR (CD1911)	This study
oMC665	5'-AAAAGCTTTTGCAACCCACGTCGATCGTGAAGGAAGGCTTGTAGTGCGCCCAGATAGGGT-3'	*eutA* intron retargeting (CD1912)	This study
oMC666	5'-CAGATTGTACAAATGTGGTGATAACAGATAAGTCCTTGTAAATAACTTACCTTTCTTTGT-3'	*eutA* intron retargeting (CD1912)	This study
oMC667	5'-CGCAAGTTTCTAATTTCGGTTCTTCCTCGATAGAGGAAAGTGTCT-3'	*eutA* intron retargeting (CD1912)	This study
oMC674	5'-AAAAGCTTTTGCAACCCACGTCGATCGTGAATCTACCTCGTTAGTGCGCCCAGATAGGGTG-3'	*eutG* intron retargeting (CD1907)	This study
oMC675	5'-CAGATTGTACAAATGTGGTGATAACAGATAAGTCTCGTTAATTAACTTACCTTTCTTTGT-3'	*eutG* intron retargeting (CD1907)	This study
oMC676	5'-CGCAAGTTTCTAATTTCGGTTGTAGATCGATAGAGGAAAGTGTCT-3'	*eutG* intron retargeting (CD1907)	This study
oMC714	5'-GGAGAAGGCTCACTAAAAGC-3'	*eutG* verification	This study
oMC715	5'-GCCTCTTTGCTTGTTTAAGAC-3'	*eutA* verification	This study
oMC716	5'-GTAGCCATTGTACCTACTTGAAG-3'	*eutA* verification	This study
oMC855	5'-TCATAGCTAACCCTAATGAAGACAT-3'	*eutS* PCR (CD1908)	This study

Primer	Sequence (5'→3')	Use/location[a]	Source or reference
oMC856	5'-GCAACATCTGCTGCTATTATTGA-3'	*eutS* PCR (CD1908)	This study
oMC857	5'-GACACTCCTGGTGAGTATATGG-3'	*eutP* PCR (CD1909)	This study
oMC858	5'-GTGTGGCATCATACACTATTGC-3'	*eutP* PCR (CD1909)	This study
oMC859	5'-TCCTAAGGATGCAGAAGCTTATTT-3'	*eutC* PCR (CD1914)	This study
oMC860	5'-CAGCATGGTCTGCTCTAAATCT-3'	*eutC* PCR (CD1914)	This study
oMC861	5'-ACTGCAGACTGTGATGATGTT-3'	*eutL* PCR (CD1915)	This study
oMC862	5'-CAGCACCTGCATACATTGATTT-3'	*eutL* PCR (CD1915)	This study
oMC863	5'-GGAGATGTCGGTGCTGTAAA-3'	*eutM* PCR (CD1916)	This study
oMC864	5'-TGTTCTTAATGTACCAACTCTGGA-3'	*eutM* PCR (CD1916)	This study
oMC865	5'-TGGTGAAGATAAGGAAGCCAATA-3'	*eutE* PCR (CD1917)	This study
oMC866	5'-GATGTTGGGTTTGTTGAAGGTATAA-3'	*eutE* PCR (CD1917)	This study
oMC867	5'-GCAGCAGATGCAATGGTTAAA-3'	*eutK* PCR (CD1918)	This study
oMC868	5'-CAGCTCCAACATCTCCTCTTAC-3'	*eutK* PCR (CD1918)	This study
oMC869	5'-TTTGGCGCTAAATTGGATGAAA-3'	*eutT* PCR (CD1919)	This study
oMC870	5'-TTCCTTAACAAGCTTTGGCATATC-3'	*eutT* PCR (CD1919)	This study
oMC871	5'-ATAGAAGTTGAAGCATCAGGAAGAC-3'	*eutD* PCR (CD1920)	This study
oMC872	5'-CATGCATATTGACCTGGTTGAGATA-3'	*eutD* PCR (CD1920)	This study
oMC873	5'-CCTAAAGCTGTGATTGTATTTGAACAAG-3'	*eut hyp* PCR (CD1921)	This study
oMC874	5'-ATTTCCAAGTGCTATATTCGATAGTCC-3'	*eut hyp* PCR (CD1921)	This study
oMC875	5'-AACTAAAGACACATACAAGGAAGGC-3'	*eutN* PCR (CD1922)	This study
oMC876	5'-TCTAGCTGAGGAACCTTTGGATATAA-3'	*eutN* PCR (CD1922)	This study
oMC877	5'-AGGCGTTGTTGAAAGTAGTAAAGT-3'	*pduT* PCR (CD1923)	This study
oMC878	5'-ACTGTCTACTGATGGTATTACAGTCT-3'	*pduT* PCR (CD1923)	This study
oMC879	5'-TGGTCTTGGAGAACAATTTGAAGA-3'	*eutH* PCR (CD1924)	This study
oMC880	5'-ATCAGCAAGAACTGGTGCTAAA-3'	*eutH* PCR (CD1924)	This study
oMC881	5'-AAGTGGAACTAAAGACACAGTAGAT-3'	*eutQ* PCR (CD1925)	This study
oMC882	5'-CCTAATCTTGGGCTTTCCTCTAAT-3'	*eutQ* PCR (CD1925)	This study
oMC972	5'-ATAAGAGCCACAGTGGTTGG-3'	*eutA* PCR (CD1912)	This study
oMC973	5'-CTGGCAAGTTCTTAAGTGGAAAC-3'	*eutA* PCR (CD1912)	This study
oMC1588	5'-GGGATTGCATATGGAAATCAATGTTATAG-3'	*CD1906* PCR	This study
oMC1589	5'-TTTACAAACCAACTAGCTTTATCCATTTC-3'	*CD1906* PCR	This study
oMC1593	5'-GGCTTTAGGAATGGTTGGTATAGTT-3'	*CD0742* PCR	This study
oMC1594	5'-CTCCACAGAGATTGAAGATTGGTATT-3'	*CD0742* PCR	This study
oMC1595	5'-AAACTAGGAGGTCTTGACAGATTAGA-3'	*CD3167* PCR	This study
oMC1596	5'-GGTCAAGGATAGTATCAAGTGCAAATA-3'	*CD3167* PCR	This study
oMC1634	5'-CTTGTTTAGCAGGTATGGCATTTAAC-3'	*eutG* (*CD1907*; 3') PCR	This study
oMC1635	5'-TTCCACCTAATACATGTGCAATAGAA-3'	*eutG* (*CD1907*; 3') PCR	This study
oMC1687	5'-GAAGTACATATGCTAACAGCGATTG-3'	*CDR20291_1847*	This study
oMC1688	5'-GAGATATTGCACCTTTAGTTCTGTTC-3'	*CDR20291_1847*	This study

Primer	Sequence (5'→3')	Use/location[a]	Source or reference
fliCqF	5'-TACAAGTTGGAGCAAGTTATGGAAC-3'	*fliC* PCR (CD0239)	(McKee et al., 2013)
fliCqR	5'-GTTGTTATACCAGCTGAAGCCATTA-3'	*fliC* PCR (CD0239)	(McKee et al., 2013)
qRTpilA1F	5'-TGGCAGTTCCAGCTTTATTTAGTAAT-3'	*pilA1* PCR (CD3513)	(Purcell et al., 2016)
qRTpilA1R	5'-AAGATAATGCTGCACTCTTAACTGAA-3'	*pilA1* PCR (CD3513)	(Purcell et al., 2016)